

International Journal of Modern Physics A
 © World Scientific Publishing Company

Mass Spectra and Decay Properties of Singly Heavy Bottom-Strange Baryons

AMEE KAKADIYA, ZALAK SHAH and AJAY KUMAR RAI

*Department of Physics, Sardar Vallabhbhai National Institute of Technology, Ichchhanath,
 Surat-395007, Gujarat, India **

We enumerated ground and excited state masses of singly heavy bottom-strange baryons using the Hypercentral Constituent Quark Model (hCQM). The screening potential is used with color-Coulomb potential, as the confining potential. We determine the possible J^P values to recently observed excited states like, $\Xi_b(6100)$, $\Xi_b(6227)$, $\Xi_b(6327)$, $\Xi_b(6333)$ and four $\Omega_b(6316, 6330, 6340, 6350)$ states. The Regge trajectories are plotted in (J, M^2) plane to assign the J^P values and quantum numbers to recently observed states. Using the calculated spectroscopic data, properties such as magnetic moment, transition magnetic moment, radiative decay width, and strong decay width are also investigated for all singly heavy bottom-strange baryonic system.

Keywords: Mass spectra; Heavy baryons; Regge trajectory; Magnetic moment; Decay width.

1. Introduction

Understanding the nature of hadrons containing bottom quarks has been accomplished over the last two decades. There have been numerous experimental¹⁻⁶ and theoretical studies⁷⁻¹² on the mass spectra and properties of heavy baryons. Many bottom baryon decay channels have been observed at various experimental facilities, and a large amount of data on heavy baryons has been gathered. The spectroscopy and properties of heavy baryons are vast and useful topics in hadronic physics. The study of heavy flavour baryons containing b or c quark can play an emergent role to get deep understanding of QCD. The singly heavy bottom-strange baryons belong to two different $SU(3)$ flavor representations: $3 \otimes 3 = 6_s \oplus \bar{3}_A$. The Ω_b baryon is a part of $SU(3)$ symmetric sextet, while Ξ_b doublet is a part of anti-symmetric anti-triplets.

$$\Omega_b^- = ssb, \Xi_b^0 = \frac{1}{\sqrt{2}}(us - su)b, \Xi_b^- = \frac{1}{\sqrt{2}}(ds - sd)b$$

Large samples of bottom baryon decays have been collected by Hadron collider experiments, allowing for increasingly precise mass and lifetime measurements. The Particle Data Group (PDG)¹ recently published a list of eleven new baryonic states in the singly heavy bottom family that have yet to be assigned a J^P values such

*ameekakadiya@gmail.com; zalak.physics@gmail.com; raiajayk@gmail.com

2 *Amee Kakadiya, Zalak Shah and Ajay Kumar Rai*Table 1. Mass, width, J^P value and experimental status of the singly heavy bottom-strange baryons from PDG.¹

Resonance	Mass (in MeV)	Width (in MeV)	Mean life (10^{-12} sec)	J^P	Status
Ξ_b^0	5791.9 ± 0.5	-	$1.477 \pm 0.026 \pm 0.019$	$\frac{1}{2}^+$	***
Ξ_b^-	5797.0 ± 0.5	-	1.57 ± 0.04	$\frac{1}{2}^+$	***
$\Xi_b'(5935)^-$	5935.02 ± 0.05	< 0.08	-	$\frac{1}{2}^+$	***
$\Xi_b(5945)^0$	5952.3 ± 0.6	0.90 ± 0.18	-	$\frac{3}{2}^+$	***
$\Xi_b(5955)^-$	5955.33 ± 0.13	23.96 ± 0.13	-	$\frac{3}{2}^+$	***
$\Xi_b(6100)^-$	6100.3 ± 0.2	< 1.9	-	$?^?$	-
$\Xi_b(6227)^0$	6226.8 ± 1.6	19^{+5}_{-4}	-	$?^?$	***
$\Xi_b(6227)^-$	6227.9 ± 0.9	19.9 ± 2.6	-	$?^?$	***
$\Xi_b(6327)^-$	$6327.3^{+0.23}_{-0.21}$	< 2.56	-	$?^?$	-
$\Xi_b(6333)^-$	$6333.3^{+0.17}_{-0.18}$	< 1.85	-	$?^?$	-
Ω_b^-	6046.1 ± 1.7	-	$1.65^{+0.18}_{-0.16}$	$\frac{1}{2}^+$	***
$\Omega_b(6316)^-$	6315.6 ± 0.6	< 4.2	-	$?^?$	*
$\Omega_b(6330)^-$	6330.3 ± 0.6	< 4.7	-	$?^?$	*
$\Omega_b(6340)^-$	6339.7 ± 0.6	< 1.8	-	$?^?$	*
$\Omega_b(6350)^-$	6349.8 ± 0.6	< 3.2	-	$?^?$	*

as, $\Lambda_b(6070)^0$, $\Sigma_b(6097)$, $\Xi_b(6100)^-$, $\Xi_b(6227)^-$, $\Xi_b(6227)^0$, $\Xi_b(6327)^0$, $\Xi_b(6333)^0$, $\Omega_b(6315)^-$, $\Omega_b(6330)^-$, $\Omega_b(6340)^-$, and $\Omega_b(6350)^-$. The list of all known singly heavy strange-bottom baryons are shown in Table 1 with the mass, width, mean life and status..

Spectroscopy of single heavy baryons is an important tool for studying the behaviour of light quarks in the presence of heavy quarks. Singly bottom baryons have been studied using a variety of theoretical and phenomenological approaches to the date, such as the Heavy Quark Symmetry (HQS),^{13–15} relativistic quark-diquark picture,¹⁶ QCD sum rule,^{17, 18} relativistic flux tube model¹⁹, Regge Phenomology,^{20, 21} Holography Inspired Stringy Hadron (HISH) model,²² non-relativistic constituent quark model,^{23–30} lattice QCD³¹ etc.

In this article, we introduce the non-relativistic approach of hypercentral Constituent Quark Model (hCQM) employing the screening potential as confining potential with color-Coulomb potential. Such a model is well established and have been used to determine the properties of heavy flavored baryons previously (see in Refs.^{32–35}). The goal of this research is to look insights into singly heavy bottom-strange baryons and assign a J^P value to experimentally observed states that don't have one, to plot the Regge trajectory (In J, M^2 plane) to justify calculated mass spectra, and to investigate their properties. The structure of this paper is as follows: Starting with the introduction in section-1, the theoretical framework is explained in section-2. The mass spectra of radial and excited states of Ξ_b , Ξ_b' , and Ω_b baryons are tabulated along with the Regge trajectories in the (J, M^2) planes in section-3. The properties of singly heavy bottom-strange baryons are presented in Section 4, including magnetic moment, transition magnetic moment, transition decay widths, and strong decay widths. Finally, summary is presented in section-5.

2. Theoretical framework

The Hypercentral Constituent Quark Model has been utilized to describe the inter-quark interaction. The screening potential³⁶ is incorporated as a confining potential with color-Coulomb potential. The Jacobi coordinates are employed to understand the the dynamics of the constituent quarks inside the baryonic system, which can be expressed as,^{37–40}

$$\vec{\rho} = \frac{\vec{r}_1 - \vec{r}_2}{\sqrt{2}} \quad \text{and} \quad \vec{\lambda} = \frac{\vec{r}_1 + \vec{r}_2 - 2\vec{r}_3}{\sqrt{6}}. \quad (1)$$

The hyper radius x is a collective variable gives a measure of dimension of the three-quark system and the hyper angle ξ reflects its deformation. We define as:⁴¹

$$x = \sqrt{\rho^2 + \lambda^2} \quad \text{and} \quad \xi = \arctan\left(\frac{\rho}{\lambda}\right) \quad (2)$$

The Hamiltonian of the three quark bound system is given by,^{41,42}

$$H = \frac{P^2}{2m} + V(x) \quad (3)$$

x is the six dimensional radial hyper central coordinate of the three body system. The expression of kinetic energy operator for the baryonic system of three quarks in center-of-mass frame is,

$$\frac{P_x^2}{2m} = -\frac{\hbar^2}{2m}(\Delta_\rho + \Delta_\lambda) = -\frac{\hbar^2}{2m} \left(\frac{\partial^2}{\partial x^2} + \frac{5}{x} \frac{\partial}{\partial x} + \frac{L^2(\Omega)}{x^2} \right) \quad (4)$$

Here, P is conjugate momentum, $L^2(\Omega) = L^2(\Omega_\rho, \Omega_\lambda, \xi)$ is the Grand angular operator, which is the six-dimensional generalization of the squared angular momentum operator. m is the reduced mass of the system, which expressed as, $m = \frac{2m_\rho m_\lambda}{m_\rho + m_\lambda}$. where, $m_\rho = \frac{2m_1 m_2}{m_1 + m_2}$ and $m_\lambda = \frac{2m_3(m_1^2 + m_2^2 + m_1 m_2)}{(m_1 + m_2)(m_1 + m_2 + m_3)}$. Here, m_1, m_2, m_3 are the masses of the constituent quarks: $m_u = m_d = 0.344 \text{ GeV}$, $m_s = 0.500 \text{ GeV}$, $m_b = 4.670 \text{ GeV}$.

$V(x)$ is non-relativistic interaction potential inside the baryonic system, which comes in two terms i.e. spin dependent (V_{SD}) and spin independent (V_{SI}) potential term.^{34,43,44}

$$V(x) = V_{SD}(x) + V_{SI}(x) \quad (5)$$

The spin dependent part of potential $V_{SD}(x)$ contains three interaction terms, which are: the spin-spin interaction term $V_{SS}(x)$, the spin-orbit interaction term $V_{\gamma S}(x)$ and tensor term $V_T(x)$,^{37,38}

$$V_{SD}(x) = V_{SS}(x)(\vec{S}_\rho \cdot \vec{S}_\lambda) + V_{\gamma S}(x)(\vec{\gamma} \cdot \vec{S}) + V_T(x) \left[S^2 - \frac{3(\vec{S} \cdot \vec{x})(\vec{S} \cdot \vec{x})}{x^2} \right] \quad (6)$$

4 *Ameeta Kakadiya, Zalak Shah and Ajay Kumar Rai*

where $\vec{S} = \vec{S}_\rho + \vec{S}_\lambda$, are the spin vector associated with the $\vec{\rho}$ and $\vec{\lambda}$ variables respectively (more details can be found in²³). The Spin-orbit and the tensor term describe the fine structure of the states, while the spin-spin term gives the spin singlet triplet splittings.

$$V_{SS}(x) = \frac{1}{3m_\rho m_\lambda} \nabla^2 V_V \quad (7)$$

$$V_{\gamma S}(x) = \frac{1}{2m_\rho m_\lambda x} \left(3 \frac{dV_V}{dx} - \frac{dV_S}{dx} \right) \quad (8)$$

$$V_T(x) = \frac{1}{6m_\rho m_\lambda} \left(3 \frac{d^2 V_V}{dx^2} - \frac{1}{x} \frac{dV_V}{dx} \right) \quad (9)$$

The screened potential is incorporated as confining potential with the color-Coulomb potential (spin independent potential $V_{SI}(x) = V_{conf}(x) + V_{Col}(x)$).³²⁻³⁵

$$V_{conf}(x) = a \left(\frac{1 - e^{-\mu x}}{\mu} \right) \quad (10)$$

where, a is the string tension and the constant $\mu(0.07 \text{ GeV})$ is the screening factor. When $x \ll \frac{1}{\mu}$, the screened potential becomes linear like potential ax and when $x \gg \frac{1}{\mu}$, it will be a constant $\frac{a}{\mu}$. Hence, it is interesting to generate the mass spectra employing screened potential, which gives the lower mass values of excited states than linear potential.^{36, 45} And the color-Coulomb potential is,

$$V_{Col}(x) = \frac{\tau}{x} \quad (11)$$

where, x indicates the inter-quark separation, the hyper-Coulomb strength $\tau = -\frac{2}{3}\alpha_s$ ($\frac{2}{3}$ is color factor for baryon), the parameter α_s corresponds to the strong running coupling constant with value 0.7.³⁹ The short-distance part of the static three-quark system, arising from one-gluon exchange within baryon, is of Coulombic shape. Here, we can observe that the strong running coupling constant (α_s) becomes smaller as we decrease the distance, the effective potential approaches the lowest order one-gluon exchange potential given as $r \rightarrow 0$. So, for short distances, one can use the one gluon exchange potential, taking into account the running coupling constant α_s .

3. Mass spectra and Regge trajectories

Masses of all possible states presented in this work, are calculated using Mathematica notebook.⁴⁶ And from the calculated masses, the J^P value can be assigned to the newly observed states which have no confirmed J^P value.

Table 2. Predicted masses of radial states of Ξ_b baryon (in GeV).

state	Present	PDG ¹	16	21	24	47	13
1S	5.796	5.797	5.803	5.793	5.806	5.795	5.806
2S	6.208			6.266			
3S	6.533			6.601			
4S	6.825			6.913			
5S	7.094			7.165			
6S	7.347			7.415			

Table 3. Predicted masses of radial states of Ξ'_b baryon (in GeV).

state	Present		PDG ¹		16		12		21
	$S = \frac{1}{2}$	$S = \frac{3}{2}$	$S = \frac{1}{2}$	$S = \frac{3}{2}$	$s = \frac{1}{2}$	$s = \frac{3}{2}$	$s = \frac{1}{2}$	$s = \frac{3}{2}$	
1S	5.935	5.958	5.935	5.955	5.936	5.963			5.935
2S	6.328	6.343			6.329	6.342	6.329	6.342	
3S	6.625	6.634			6.687	6.695			
4S	6.902	6.907			6.978	6.984			
5S	7.161	7.165			7.229	7.234			
6S	7.405	7.408							

3.1. Ξ_b State

One u/d quark, one s quark, and one bottom quark make up the Ξ_b baryons. The Ξ_b baryon exists in three states: $\Xi_b^0(usb)$, $\Xi_b^-(dsb)$, and $\Xi_b'^-(dsb)$. (Even though the quark composition is identical, Ξ_b^- and $\Xi_b'^-$ are distinct.) Three such Ξ_b isodoublets are expected to exist, none of which are orbitally or radially excited, and which can be classified by the spin j of the us or ds light di-quark and the spin-parity J^P of the baryon: one with $j = 0$ and $J^P = \frac{1}{2}^+$ (Ξ_b), one with $j = 1$ and $J^P = \frac{1}{2}^+$ (Ξ_b'), one with $j = 1$ and $J^P = \frac{3}{2}^+$ (Ξ_b^*), follows the same pattern as the well-known Ξ_c states,⁴⁸ and we therefore refer to these three iso-doublets as the Ξ_b , the Ξ_b' and Ξ_b^* . The spin-antisymmetric $J^P = \frac{1}{2}^+$ state, observed by multiple experiments¹ others should decay predominantly strongly through a P -wave pion transition ($\Xi_b'^* \rightarrow \Xi_b \pi$) if their masses are above the kinematic threshold for such a decay; otherwise they should decay electromagnetically ($\Xi_b'^* \rightarrow \Xi_b \gamma$).⁴⁹

The new excited state $\Xi_b^-(6227)$ is also detected by LHCb collaboration.³ Three Ξ_b excited states are also detected during proton-proton (pp) collision at the LHC at $\sqrt{13} = \text{TeV}$, which are, $\Xi_b^-(6100)^-$, $\Xi_b^-(6327)^0$ and $\Xi_b^-(6333)^0$.^{5,6}

The masses of radial states of Ξ_b and Ξ_b' baryons are listed in Table 2 and 3, and the masses of orbital states of Ξ_b and Ξ_b' baryons are listed in Table 4 and 5. 2S state is lesser by 55-60 MeV from Ref.¹⁶ and it will decrease with increment of principal quantum number. For 1P state, there is a few MeV difference with Ref.,¹⁶ but for higher excited orbital states, the difference is increasing as 120-140 MeV for 1D state and around 300 MeV for 1F state. The new state $\Xi_b(6227)^{0,-}$,

6 Ameer Kakadiya, Zalak Shah and Ajay Kumar Rai

Table 4. Predicted masses of orbital excited states of Ξ_b baryon (in GeV).

state	$2S+1$	J^P	Present	Exp. ^{5,6}	16	14	24	47	19	20
1P	2	$\frac{1}{2}^-$	6.137		6.120	6.054	6.090	6.106	6.097	
		$\frac{3}{2}^-$	6.135	6.100	6.130	6.040	6.093	6.115	6.106	6.093
		$\frac{5}{2}^-$								
	4	$\frac{1}{2}^-$	6.138			6.079				
		$\frac{3}{2}^-$	6.136							
		$\frac{5}{2}^-$	6.133							6.240
2P	2	$\frac{1}{2}^-$	6.341		6.496					
		$\frac{3}{2}^-$	6.339		6.502					
		$\frac{5}{2}^-$								
	4	$\frac{1}{2}^-$	6.342							
		$\frac{3}{2}^-$	6.340							
		$\frac{5}{2}^-$	6.338							
3P	2	$\frac{1}{2}^-$	6.520		6.805					
		$\frac{3}{2}^-$	6.519		6.810					
		$\frac{5}{2}^-$								
	4	$\frac{1}{2}^-$	6.521							
		$\frac{3}{2}^-$	6.520							
		$\frac{5}{2}^-$	6.518							
4P	2	$\frac{1}{2}^-$	6.679		7.068					
		$\frac{3}{2}^-$	6.678		7.073					
		$\frac{5}{2}^-$								
	4	$\frac{1}{2}^-$	6.679							
		$\frac{3}{2}^-$	6.678							
		$\frac{5}{2}^-$	6.677							
1D	2	$\frac{3}{2}^+$	6.243	6.327	6.366			6.344		
		$\frac{5}{2}^+$	6.240	6.333	6.373			6.349		6.380
		$\frac{7}{2}^+$								
	4	$\frac{1}{2}^+$	6.247							
		$\frac{3}{2}^+$	6.245							
		$\frac{5}{2}^+$	6.241							
2D	2	$\frac{3}{2}^+$	6.237							6.516
		$\frac{5}{2}^+$								
		$\frac{7}{2}^+$								
	4	$\frac{1}{2}^+$	6.438		6.690					
		$\frac{3}{2}^+$	6.436		6.696					
		$\frac{5}{2}^+$	6.440							
3D	2	$\frac{1}{2}^+$	6.439							
		$\frac{3}{2}^+$	6.437							
		$\frac{5}{2}^+$	6.434							
	4	$\frac{1}{2}^+$	6.610		6.966					
		$\frac{3}{2}^+$	6.608		6.970					
		$\frac{5}{2}^+$	6.611							
4D	2	$\frac{1}{2}^+$	6.610							
		$\frac{3}{2}^+$	6.609							
		$\frac{5}{2}^+$	6.607							
	4	$\frac{1}{2}^+$	6.762		7.208					
		$\frac{3}{2}^+$	6.761		7.212					
		$\frac{5}{2}^+$	6.763							
5D	2	$\frac{1}{2}^+$	6.763							
		$\frac{3}{2}^+$	6.763							
		$\frac{5}{2}^+$	6.762							
	4	$\frac{1}{2}^+$	6.762							
		$\frac{3}{2}^+$	6.761							
		$\frac{5}{2}^+$	6.761							

Table 4. (Continued)

state	$2S + 1$	JP	Present	PDG ¹	16	14	24	47	19	20
1F	2	$\frac{5}{2}^-$	6.336		6.577			6.555		
		$\frac{7}{2}^-$	6.331		6.581			6.559		6.654
	4	$\frac{3}{2}^-$	6.341							
		$\frac{5}{2}^-$	6.337							
		$\frac{7}{2}^-$	6.333							
		$\frac{9}{2}^-$	6.328							6.780
		$\frac{5}{2}^-$								
		$\frac{7}{2}^-$								
2F	2	$\frac{5}{2}^-$	6.524		6.863					
		$\frac{7}{2}^-$	6.521		6.867					
	4	$\frac{3}{2}^-$	6.527							
		$\frac{5}{2}^-$	6.524							
		$\frac{7}{2}^-$	6.522							
		$\frac{9}{2}^-$	6.519							
		$\frac{5}{2}^-$								
		$\frac{7}{2}^-$								
		$\frac{9}{2}^-$								

$\Xi_b(6100)^-$, $\Xi_b(6327)^0$ and $\Xi_b(6333)^0$ is compatible for $2S_{\frac{1}{2}^+}$, $1P_{\frac{3}{2}^-}$, $1D_{\frac{3}{2}^+}$ and $1D_{\frac{5}{2}^+}$ respectively, as per our calculation and it is shown with bold numbers in Table 2 and 3. By CMS collaboration, $\Xi_b(6100)^-$ state is predicted as $1P(\frac{3}{2}^-)$ ⁶ and the narrow doublet $\Xi_b(6327)^0$ and $\Xi_b(6333)^0$ are predicted as $1D(\frac{3}{2}^+)$ and $1D(\frac{5}{2}^+)$ by LHCb collaboration.⁵ Azizi⁸ studied the resonance $\Xi_b(6227)^-$ and conclude that the resonance may be $2S$ or $1P$ excited state of Ξ_b . And He, Liang et. al.¹² concluded that $\Xi_b(6227)^-$ may be $1P(\frac{3}{2}^-)$ of Ξ'_b . As $\Xi_b(6100)$ is defined $1P$ state,⁶ $\Xi_b(6227)^-$ state must be $2S$ state. For $\Xi_b'^-$ baryon, $1S$ and $2S$ states are quite near to the Refs.¹² and²¹. Our masses $1P$ state is in good agreement with Ref.²¹ and 93 MeV differ from Ref.¹⁴ $1D$ and $1F$ states are in decrements of around 100 MeV and 250 MeV from Refs.¹² and²¹ due to screening effect. The suppression of our calculated mass from the other theoretical predictions is showing the screening effect. The Ξ_b^0 and Ξ_b^- are very narrow states, they are considered as single state by taking the average of constituent quark masses of u and d quarks.

3.2. Ω_b^- State

Ω_b is the heaviest member of the singly bottom family, consist of one bottom (heavy) quark and two strange (light) quarks with strangeness of -2. The measurements of the mass and lifetime of the Ω_b^- baryon have been done using the various decay modes. The Ω_b^- baryon detected by LHCb collaboration,⁵² CDF collaboration⁵³ and D0 collaboration⁵⁴ (Fermi lab). The radial and orbital masses of Ω_b baryon is listed in Table 8 and 9 respectively. The mass of $1S$ state of Ω_b^- is quite near to the compared Refs.^{10, 11, 16, 21} with difference of 5-50 MeV. The masses of $2S - 6S$ states are also near to the Refs.^{10, 11, 16, 21}

8 *Amee Kakadiya, Zalak Shah and Ajay Kumar Rai*Table 5. Predicted masses of orbital excited states of Ξ'_b baryon (in GeV).

state	$2S + 1$	J^P	Present	PDG ¹	16	12	21	14	10	20
1P	2	$\frac{1}{2}^-$	6.235	6.227	6.233	6.233		6.142	6.226	6.229
		$\frac{3}{2}^-$	6.232		6.234	6.234	6.215	6.093	6.243	
	4	$\frac{1}{2}^-$	6.237		6.227	6.227		6.176	6.235	
		$\frac{3}{2}^-$	6.234		6.224	6.224			6.252	
		$\frac{5}{2}^-$	6.229		6.226	6.226			6.262	
2P	2	$\frac{1}{2}^-$	6.494		6.611					
		$\frac{3}{2}^-$	6.492		6.605					
	4	$\frac{1}{2}^-$	6.495		6.604					
		$\frac{3}{2}^-$	6.493		6.598					
		$\frac{5}{2}^-$	6.490		6.596					
3P	2	$\frac{1}{2}^-$	6.731		6.915					
		$\frac{3}{2}^-$	6.729		6.905					
	4	$\frac{1}{2}^-$	6.732		6.906					
		$\frac{3}{2}^-$	6.730		6.900					
		$\frac{5}{2}^-$	6.728		6.897					
4P	2	$\frac{1}{2}^-$	6.949		7.174					
		$\frac{3}{2}^-$	6.948		7.163					
	4	$\frac{1}{2}^-$	6.950		7.164					
		$\frac{3}{2}^-$	6.949		7.159					
		$\frac{5}{2}^-$	6.947		7.156					
1D	2	$\frac{1}{2}^+$	6.375		6.459	6.459				
		$\frac{3}{2}^+$	6.371		6.432	6.432	6.486			
	4	$\frac{1}{2}^+$	6.380		6.447	6.447				
		$\frac{3}{2}^+$	6.377		6.431	6.431				
		$\frac{5}{2}^+$	6.373		6.420	6.420				6.510
2D	2	$\frac{1}{2}^+$	6.368		6.414	6.414				
		$\frac{3}{2}^+$	6.628		6.775					
	4	$\frac{1}{2}^+$	6.625		6.751					
		$\frac{3}{2}^+$	6.632		6.767					
		$\frac{5}{2}^+$	6.630		6.751					
3D	2	$\frac{1}{2}^+$	6.626		6.740					
		$\frac{3}{2}^+$	6.621		6.736					
	4	$\frac{1}{2}^+$	6.859		6.856					
		$\frac{3}{2}^+$	6.861		6.860					
		$\frac{5}{2}^+$	6.857		6.854					
4D	2	$\frac{1}{2}^+$	7.070		7.069					
		$\frac{3}{2}^+$	7.072		7.071					
	4	$\frac{1}{2}^+$	7.069		7.067					
		$\frac{3}{2}^+$								
		$\frac{5}{2}^+$								

Table 7. (Continued)

Mass spectroscopy and decay properties of singly heavy bottom-strange baryons 9

state	$2S + 1$	J^P	Present	16	12	21	14	20
1F	2	$\frac{5}{2}^-$	6.501	6.686				
		$\frac{7}{2}^-$	6.495	6.640		6.745 ± 0.049		
	4	$\frac{3}{2}^-$	6.509	6.675				
		$\frac{5}{2}^-$	6.503	6.640				
		$\frac{7}{2}^-$	6.497	6.619				6.779
		$\frac{9}{2}^-$	6.489	6.610				
		$\frac{11}{2}^-$						
2F	2	$\frac{5}{2}^-$	6.747					
		$\frac{7}{2}^-$	6.744					
	4	$\frac{3}{2}^-$	6.752					
		$\frac{5}{2}^-$	6.749					
		$\frac{7}{2}^-$	6.745					
		$\frac{9}{2}^-$	6.740					
		$\frac{11}{2}^-$						

Table 6. Predicted masses of radial states of Ω_b baryon (in GeV).

state	Present		PDG ¹	16		13		10	11	21
	$S = \frac{1}{2}$	$S = \frac{3}{2}$		$S = \frac{1}{2}$	$S = \frac{3}{2}$	$S = \frac{1}{2}$	$S = \frac{3}{2}$			
1S	6.046	6.082	6.046	6.064	6.088	6.081	6.102	6.051	6.098	6.048
2S	6.438	6.462		6.450	6.461	6.472	6.478	6.489		
3S	6.740	6.753		6.804	6.811	6.593	6.593			
4S	7.022	7.030		7.091	7.096					
5S	7.290	7.296		7.338	7.343					
6S	7.546	7.549								

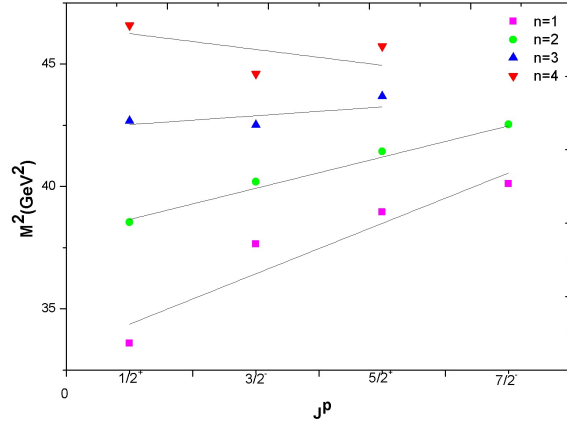
For $1P$ states, our calculated masses are in accordance with the newly detected four narrow states. We assigned the J^P values to the states, which are shown with bold in Table 7. One of the four newly observed narrow states, $\Omega_b(6316)$ can be assigned as $1^2P_{\frac{3}{2}}$, which is 25 MeV lesser than our calculated mass for the particular state. The other three states, $\Omega_b(6330)$, $\Omega_b(6340)$ and $\Omega_b(6350)$ can be assigned as further hyperfine states of $1P$, and they are 11 MeV, 5 MeV and 3 MeV differ from our calculated masses respectively. These narrow states are also defined by Z. G. Wang¹⁷ as: $\Omega_b(6316) \rightarrow 1P(\frac{3}{2}^-)$, $\Omega_b(6330) \rightarrow 1P(\frac{1}{2}^-)$, $\Omega_b(6340) \rightarrow 1P(\frac{5}{2}^-)$ and $\Omega_b(6350) \rightarrow 1P(\frac{3}{2}^-)$, using full QCD sumrules. Our results are also matching with Refs.^{15, 16} and as the principal quantum number increases, our results are suppressed around 200 MeV from the compared theoretical predictions due to screening effect. The similar effect can be observed for D and F state also.

10 *Amees Kakadiya, Zalak Shah and Ajay Kumar Rai*Table 7. Predicted masses of orbital excited states of Ω_b baryon (in GeV).

state	$2S+1$	J^P	Present	PDG ¹	16	15	10	21	14	28	20
1P	2	$\frac{1}{2}^-$	6.344	6.330	6.339	6.314	6.342		6.248		
		$\frac{3}{2}^-$	6.341	6.316	6.340	6.330		6.325	6.207		6.348
	4	$\frac{1}{2}^-$	6.345		6.330	6.339			6.269	6.333	
		$\frac{3}{2}^-$	6.343	6.350	6.331	6.342				6.336	
		$\frac{5}{2}^-$	6.339	6.340	6.334	6.352				6.345	6.362
		$\frac{7}{2}^-$									
2P	2	$\frac{1}{2}^-$	6.596		6.710		6.724				
		$\frac{3}{2}^-$	6.594		6.705						
	4	$\frac{1}{2}^-$	6.597		6.706					6.740	
		$\frac{3}{2}^-$	6.595		6.699					6.744	
		$\frac{5}{2}^-$	6.592		6.700					6.728	
		$\frac{7}{2}^-$									
3P	2	$\frac{1}{2}^-$	6.829		7.009						
		$\frac{3}{2}^-$	6.827		7.003						
	4	$\frac{1}{2}^-$	6.830		7.002					6.937	
		$\frac{3}{2}^-$	6.828		6.998					6.937	
		$\frac{5}{2}^-$	6.826		6.996					6.919	
		$\frac{7}{2}^-$									
4P	2	$\frac{1}{2}^-$	7.044		7.265						
		$\frac{3}{2}^-$	7.043		7.258						
	4	$\frac{1}{2}^-$	7.043		7.257						
		$\frac{3}{2}^-$	7.043		7.250						
		$\frac{5}{2}^-$	7.042		7.251						
		$\frac{7}{2}^-$									
1D	2	$\frac{3}{2}^+$	6.480		6.549		6.593				6.629
		$\frac{5}{2}^+$	6.476		6.529			6.590		6.561	
	4	$\frac{1}{2}^+$	6.485		6.540						
		$\frac{3}{2}^+$	6.482		6.530						
		$\frac{5}{2}^+$	6.478		6.520						6.638
		$\frac{7}{2}^+$	6.472		6.517						
2D	2	$\frac{3}{2}^+$	6.726		6.863		6.936				
		$\frac{5}{2}^+$	6.723		6.846					6.866	
	4	$\frac{1}{2}^+$	6.730		6.857						
		$\frac{3}{2}^+$	6.727		6.846						
		$\frac{5}{2}^+$	6.724		6.837						
		$\frac{7}{2}^+$	6.720		6.834						
3D	2	$\frac{3}{2}^+$	6.953								
		$\frac{5}{2}^+$	6.951								
	4	$\frac{1}{2}^+$	6.956								
		$\frac{3}{2}^+$	6.954								
		$\frac{5}{2}^+$	6.951								
		$\frac{7}{2}^+$	6.948								
4D	2	$\frac{3}{2}^+$	7.164								
		$\frac{5}{2}^+$	7.162								
	4	$\frac{1}{2}^+$	7.166								
		$\frac{3}{2}^+$	7.164								
		$\frac{5}{2}^+$	7.162								
		$\frac{7}{2}^+$	7.160								

Table 9. (Continued)

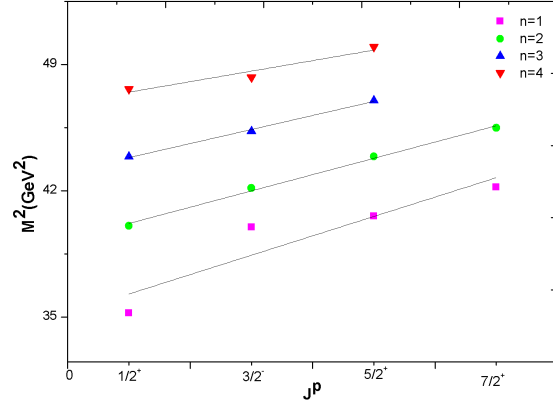
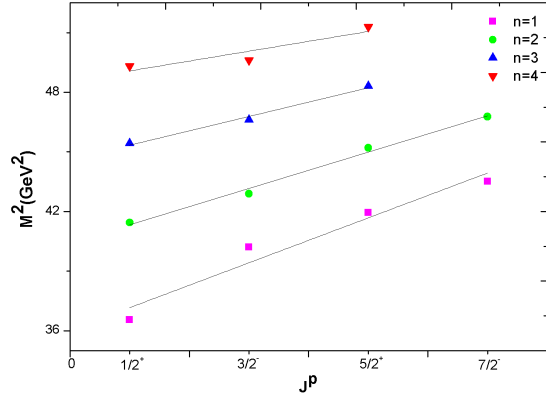
state	$2S+1$	J^P	Present	16	15	10	21	14	28	20
1F	2	$\frac{5}{2}^-$	6.602		6.771		6.817			
		$\frac{7}{2}^-$	6.596		6.736			6.844		
	4	$\frac{3}{2}^-$	6.609		6.763					
		$\frac{5}{2}^-$	6.604		6.737					
		$\frac{7}{2}^-$	6.597		6.719					6.899
		$\frac{9}{2}^-$	6.590		6.713					6.903
		$\frac{5}{2}^-$	6.843				7.132			
		$\frac{7}{2}^-$	6.839							
2F	2	$\frac{3}{2}^-$	6.848							
		$\frac{5}{2}^-$	6.845							
	4	$\frac{7}{2}^-$	6.840							
		$\frac{9}{2}^-$	6.835							
		$\frac{5}{2}^-$								
		$\frac{7}{2}^-$								

Fig. 1. Regge trajectory of Ξ_b baryon in (J, M^2) plane

3.3. Regge Trajectories

The Regge trajectories are plotted for Ξ_b , Ξ_b' and Ω_b baryons. The trajectories are drawn in the (J, M^2) plane using calculated masses for baryonic systems. The linearity of the Regge trajectories is a useful probe for predicting the masses of higher excited states, as well as for defining quantum number if the resonance mass is known. The Regge trajectories have been plotted for the states $J^P = \frac{1}{2}^+, \frac{3}{2}^-, \frac{5}{2}^+$ and $\frac{7}{2}^-$ using the equation,¹⁶

$$J = \alpha M^2 + \alpha_0 \quad (12)$$

Fig. 2. Regge trajectory of Ξ'_b baryon in (J, M^2) planeFig. 3. Regge trajectory of Ω_b baryon in (J, M^2) plane

The Regge trajectories of Ξ_b , Ξ'_b and Ω_b are shown in Figure 1, 2 and 3 respectively. Regge trajectories of Ξ_b baryons are linear but the Regge lines intersect each other for higher states which shows the effect of screened potential.

4. Properties

4.1. Magnetic Moments

The magnetic moment of a baryon is an intrinsic property caused by the spin of its constituents. The effective mass of the ground state, individual charge, and spin-flavor arrangement of the constituent quarks are used to calculate the magnetic

moment of the ground state of the singly heavy bottom-strange baryon. The expression of magnetic moment of baryon can be obtained by operating the expectation value equation,⁵⁹

$$\mu_B = \sum_q \langle \Phi_{sf} | \hat{\mu}_{qz} | \Phi_{sf} \rangle; \quad q = u, d, b \quad (13)$$

where, Φ_{sf} is the spin-flavor wave-function of the baryon and $\hat{\mu}_{qz}$ is the magnetic moment operator. The magnetic moment of individual quark is given by,⁵⁷

$$\mu_q = \frac{e_q}{2m_q^{eff}} \cdot \sigma_q \quad (14)$$

where, e_q and σ_q are charge and spin of the individual constituent quark of the baryonic system respectively and m_q^{eff} is the effective mass of constituent quark. The magnetic moment of ground states of all baryonic systems are being calculated and shown in the Table 8. Our results are also compared with different approaches. The obtained values are differ only by 0.1 to 0.5 μ_N (nuclear magneton) from Ref.⁵⁷

Table 8. Magnetic moment of ground state of singly heavy strange bottom baryons (in μ_N).

Baryon	J^P	Expression	Present	57	58	26	59	60	61
Ξ_b^0	$\frac{1}{2}^+$	$\frac{2}{3}\mu_u + \frac{2}{3}\mu_s - \frac{1}{3}\mu_b$	0.798	0.799	-0.062	-	-	-0.100	-0.110
Ξ_b^-	$\frac{1}{2}^+$	$\frac{2}{3}\mu_d + \frac{2}{3}\mu_s - \frac{1}{3}\mu_b$	-0.963	-0.958	-0.062	-	-	-0.063	-0.050
$\Xi_b'^-$	$\frac{1}{2}^+$	$\frac{2}{3}\mu_d + \frac{2}{3}\mu_s - \frac{1}{3}\mu_b$	-0.941		-0.913	-	-		
Ω_b^-	$\frac{1}{2}^+$	$\frac{4}{3}\mu_s - \frac{1}{3}\mu_b$	-0.761	-0.752	-0.741	-	-	-0.545	-0.790
Ξ_b^{*0}	$\frac{3}{2}^+$	$\mu_u + \mu_s + \mu_b$	1.101	1.083	1.031	1.136	1.041	0.690	1.190
Ξ_b^{*-}	$\frac{3}{2}^+$	$\mu_d + \mu_s + \mu_b$	-1.499	-1.505	-1.454	-1.621	-1.095	-1.088	-1.600
Ξ_b^{*-}	$\frac{3}{2}^+$	$\mu_d + \mu_s + \mu_b$	-1.498						
Ω_b^{*-}	$\frac{3}{2}^+$	$2\mu_s + \mu_b$	-1.236	-1.222	-1.201	-1.380	-1.199	-0.919	-1.280

4.2. Radiative Decays

The higher energy baryonic state decays into lower energy state, there is an emission of γ radiation. The decay width for this radiative transition is³⁷,

$$\Gamma = \frac{k^3}{4\pi} \frac{2}{2J+1} \frac{e^2}{2m_p^2} \mu_{B \rightarrow B'}^2 \quad (15)$$

where, k is photon energy, J is total angular momentum of the initial baryonic state, m_p is the mass of proton (in MeV) and $\mu_{B \rightarrow B'}$ is transition magnetic moment for the particular radiative decay (B is initial baryonic state and B' is final baryonic state).

The transition magnetic moment is expressed as,

$$\mu_{B \rightarrow B'} = \langle \Phi_B | \mu_{B \rightarrow B'} | \Phi_{B'} \rangle \quad (16)$$

Table 9. Radiative Transition magnetic moment

Transition	Expression	Present	ecqm ⁵⁷	cqm ⁵⁷
$\Xi_b^{*0} \rightarrow \Xi_b^0 \gamma$	$\frac{\sqrt{2}}{\sqrt{3}}(\mu_u - \mu_s)$	1.896	1.036	1.222
$\Xi_b^{*-} \rightarrow \Xi_b^- \gamma$	$\frac{\sqrt{2}}{\sqrt{3}}(\mu_d - \mu_s)$	-0.230	-0.124	-0.147
$\Xi_b^{*-} \rightarrow \Xi_b^{\prime -} \gamma$	$\frac{\sqrt{2}}{\sqrt{3}}(\mu_d - \mu_s)$	-0.227		
$\Omega_b^{*-} \rightarrow \Omega_b^- \gamma$	$\frac{\sqrt{2}}{3}(\mu_s - \mu_b)$	-0.246	-0.523	-0.632

Table 10. Radiative decay width

Transition	Expression	Present	ecqm ⁵⁷	cqm ⁵⁷
$\Xi_b^{*0} \rightarrow \Xi_b^0 \gamma$	$\frac{\sqrt{2}}{\sqrt{3}}(\mu_u - \mu_s)$	71.04	18.79	26.14
$\Xi_b^{*-} \rightarrow \Xi_b^- \gamma$	$\frac{\sqrt{2}}{\sqrt{3}}(\mu_d - \mu_s)$	0.99	0.09	0.13
$\Xi_b^{*-} \rightarrow \Xi_b^{\prime -} \gamma$	$\frac{\sqrt{2}}{\sqrt{3}}(\mu_d - \mu_s)$	0.22		
$\Omega_b^{*-} \rightarrow \Omega_b^- \gamma$	$\frac{\sqrt{2}}{3}(\mu_s - \mu_b)$	0.01	0.03	0.04

Here, Φ_B and Φ'_B are the wave functions of initial and final baryonic states respectively. The transition magnetic moment and radiative decay widths are listed in Table 9 and 10. Our results for transition magnetic moment and transition decay width are in range of the results shown in Ref.⁵⁷ As the $\Xi_b^{\prime -}$ baryon is not much explored, there is no data to compare for its properties like magnetic moment, transition magnetic moment and radiative decay width.

4.3. Strong Decays

The singly strange bottom baryons contains one bottom quark(b), one strange quark(s) and one of the two light quarks(u and d). This structure gives an important ground for testing the heavy quark symmetry of the bottom quark(heavy quark) and the chiral symmetry of the light quarks, due to this fact strong decays of these baryons are studied in the framework of the heavy hadron chiral perturbation theory (HHChPT).^{62–65}

Strong decay transitions are categorized in three ways according to its initial and final states: P -wave transition, S -wave transition and D -wave transition. The decay widths for P -wave, S -wave and D -wave transitions have been calculated in this work using the Lagrangian given in Ref.;⁶² where, P -wave transition is transition between s -wave baryons, S -wave transition is transition between p -wave ($J^P = \frac{1}{2}$) to s -wave baryons and D -wave transition is transition between p -wave ($J^P = \frac{3}{2}, \frac{5}{2}$) to s -wave baryons.

The expression of the decay width for P -wave transitions $\Xi_b^0(1^2S_{\frac{3}{2}}) \rightarrow \Xi_b^0\pi$,

$\Xi_b^-(1^2S_{\frac{3}{2}}) \rightarrow \Xi_b^-\pi$ and $\Xi_b'^-(1^2S_{\frac{3}{2}}) \rightarrow \Xi_b^-\pi$ respectively is,⁶³

$$\Gamma = \frac{a_1^2}{8\pi f_\pi^2} \frac{M_{\Xi_b^{0,-}}}{M_{\Xi_b^{0,-}}(1^2S_{\frac{3}{2}})} p_\pi^3 \quad (17)$$

And the expressions of the decay width for P -wave transitions $\Xi_b^0(1^2S_{\frac{3}{2}}) \rightarrow \Xi_b^-\pi$, $\Xi_b^-(1^2S_{\frac{3}{2}}) \rightarrow \Xi_b^0\pi$ and $\Xi_b'^-(1^2S_{\frac{3}{2}}) \rightarrow \Xi_b^0\pi$ respectively is,⁶³

$$\Gamma = \frac{a_1^2}{4\pi f_\pi^2} \frac{M_{\Xi_b^{-,0}}}{M_{\Xi_b^{0,-}}(1^2S_{\frac{3}{2}})} p_\pi^3 \quad (18)$$

where, strong coupling constant $a_1 = 0.565$,⁶³ the pion decay constant $f_\pi = 132$ MeV. Masses of initial and final baryon state have been taken as shown in Section 3. p_π^3 represents the P -wave transition momentum⁶⁴ (for two body decay $x \rightarrow y + \pi/K$) which can be expressed as,

$$p_{\pi/K} = \frac{1}{2m_x} \sqrt{[m_x^2 - (m_y + m_\pi/m_K)^2][m_x^2 - (m_y - m_\pi/m_K)^2]} \quad (19)$$

The expression of decay width for S -wave transition $\Xi_b^0(1^2P_{\frac{1}{2}}) \rightarrow \Xi_b'^-\pi$,

$$\Gamma = \frac{b_1^2}{4\pi f_\pi^2} \frac{M_{\Xi_b'^-}}{M_{\Xi_b^0(1^2P_{\frac{1}{2}})}} E_\pi^2 p_\pi \quad (20)$$

The decay width for S -wave transition $\Omega_b^-(1^2P_{\frac{1}{2}}) \rightarrow \Xi_b^0 K^-$ is,

$$\Gamma = \frac{b_2^2}{4\pi f_\pi^2} \frac{M_{\Xi_b^0}}{M_{\Omega_b^-(1^2P_{\frac{1}{2}})}} E_K^2 p_K \quad (21)$$

For this transition, $b_2 = \sqrt{3}b_1$ ⁶⁴ and $b_1 = 0.553$ ⁶⁴ for this particular transition.

The expression of decay width for D -wave transition $\Xi_b^0(1^2P_{\frac{3}{2}}) \rightarrow \Xi_b^{*0}\pi$ is,

$$\Gamma = \frac{b_1^2}{8\pi f_\pi^2} \frac{M_{\Xi_b^{*0}}}{M_{\Xi_b^0(1^2P_{\frac{3}{2}})}} E_\pi^2 p_\pi \quad (22)$$

And for D -wave transition $\Xi_b^0(1^2P_{\frac{3}{2}}) \rightarrow \Xi_b^{*-}\pi$,

$$\Gamma = \frac{b_1^2}{4\pi f_\pi^2} \frac{M_{\Xi_b^{*-0}}}{M_{\Xi_b^-(1^2P_{\frac{3}{2}})}} E_\pi^2 p_\pi \quad (23)$$

Here, the coupling constant $b_1 = 0.63$,⁶⁵ p_π presents S -wave transition momentum and $E_\pi \approx m_\pi$ for the single pion at rest.

Table 11. Strong decay widths of singly heavy bottom-strange baryons.

Decay channel	decay width (in MeV)	56	55	18
<i>P-wave transitions</i>				
$\Xi_b^{*0} \rightarrow \Xi_b^0 + \pi^0$	0.339	0.20		1.3
$\Xi_b^{*0} \rightarrow \Xi_b^- + \pi^+$	0.398		$2.4^{+0.1}_{-0.2}$	
$\Xi_b^{*-} \rightarrow \Xi_b^- + \pi^0$	0.265	0.40		1.3
$\Xi_b^{*-} \rightarrow \Xi_b^0 + \pi^-$	0.839		$2.4^{+0.1}_{-0.2}$	
$\Xi_b^{*-} \rightarrow \Xi_b^- + \pi^0$	0.365			
$\Xi_b^{*-} \rightarrow \Xi_b^0 + \pi^-$	1.077			
<i>S-wave Transitions</i>				
$\Xi_b^0(1P) \rightarrow \Xi_b^- + \pi^+$	4.469			
$\Xi_b^0(1P) \rightarrow \Xi_b^0 + \pi^0$	1.783			
$\Xi_b^0(1P) \rightarrow \Xi_b^{*-} + \pi^+$	3.399			
$\Omega_b^-(1P) \rightarrow \Xi_b^0 + \bar{K}^-$	445.1			
<i>D-wave transitions</i>				
$\Xi_b^-(1P) \rightarrow \Xi_b^- + \pi^0$	1.517			
$\Omega_b^-(1P) \rightarrow \Xi_b^0 + \bar{K}^-$	0.489			

The expression of decay width for D -wave transitions $\Xi_b^-(1^2P_{\frac{3}{2}}) \rightarrow \Xi_b^- \pi$ and $\Omega_b^-(1^2P_{\frac{3}{2}}) \rightarrow \Xi_b^0 K^-$ is ,

$$\Gamma = \frac{4b_3^2}{15\pi f_\pi^2} \frac{M_{\Xi_b^-,0}}{M_{\Xi_b^-(1^2P_{\frac{3}{2}})/\Omega_b^-(1^2P_{\frac{3}{2}})}} p_{\pi/K}^5 \quad (24)$$

here, coupling constant $b_3^{63,64}=0.4 \times 10^{-3} MeV^{-1}$ and $p_{\pi/K}^5$ presents D -wave transition momentum for pion or kaon.

The calculated decay widths for P -wave, S -wave and D -wave transitions of singly bottom-strange baryons have been listed in Table 11 comparing with other references.

5. Summary

The Hypercentral Constituent Quark Model(hCQM) was used to calculate the masses of radial and orbital states of singly heavy bottom-strange baryons. The color-Coulomb potential has been taken along with the confining screening potential. The calculated mass spectra are compared with various approaches and our results are in agreement with them with few MeV mass difference. In general, masses of radial (1S-3S) states and $1P$ state are close to other theoretical predictions. The screening effect can be seen at higher excited states due to the screened potential (confining potential). Above the $2P$ state, screening of 100 MeV or higher are observed in all baronic systems. Screening effect is also visible from the Regge trajectories (Figs. 1-3) for higher spin states.

- (1) The ground state masses of spin states $\frac{1}{2}$ and $\frac{3}{2}$ are in good agreement with the

experimental as well as the other theoretical predictions for all bottom strange baryons (See Table 2, 3 and 6).

- (2) In terms of assigning J^P values, the resonance state $\Xi_b(6227)^{0,-}$ corresponds to our Ξ'_b baryon 1P state with $(\frac{3}{2}^-)$. Also, $\Xi_b(6100)^-$ is assigned as $1P(\frac{3}{2}^-)$, $\Xi_b(6327)^0$ is assigned as $1D(\frac{3}{2}^+)$ and $\Xi_b(6333)^0$ is assigned as $1D(\frac{5}{2}^+)$ state with mass difference of 35 MeV, 84 MeV and 93 MeV respectively, with experimental masses. The difference between our predicted data and the experimentally observed resonance in 1D doublet is around 90 MeV, which is due to screening effect in higher orbital quantum number states.
- (3) Two states $\Omega_b^-(6316)$ and $\Omega_b^-(6330)$ are identified as (spin 1/2) $1P(\frac{3}{2}^-)$ and $1P(\frac{1}{2}^-)$ states with mass difference of 25 MeV and 14 MeV respectively. Other two states $\Omega_b^-(6350)$ and $\Omega_b^-(6340)$ identified as (Spin 3/2) $1P(\frac{3}{2}^-)$ and $1P(\frac{5}{2}^-)$ states with the mass difference of 7 MeV and 1 MeV respectively.
- (4) $\chi^2/\text{d.o.f}$ or the goodness of fit test is a statistical test, which gives an idea how near our predicted mass values to experimental values or true values. As the value of $\chi^2/\text{d.o.f}$ is large, our predicted masses contain large uncertainty and the theoretical model is not fit for the calculation and the small value of $\chi^2/\text{d.o.f}$ indicates the small uncertainty. The goodness of fit test performed as per the expression: $\frac{\chi^2}{\text{d.o.f}} = \Sigma \left(\frac{(\text{observed} - \text{experimental})^2}{\text{experimental}} \right)$.⁶⁶ In this work, the value of $\chi^2/\text{d.o.f}$ is 2.743×10^{-3} for Ξ_b , 4.015×10^{-6} for Ξ'_b and 1.299×10^{-4} for Ω_b . From the given values of $\chi^2/\text{d.o.f}$ for Ξ_b and Ω_b , it can be concluded that our data has less uncertainty and the model is perfectly fit for our calculation.
- (5) The magnetic moments and transition magnetic moments of singly heavy bottom-strange baryons are calculated in constituent quark model. Magnetic moments of all baryons are reasonably close to Ref.,⁵⁷ but not same in case of transition magnetic moment.
- (6) The strong decay width of various channels (P-wave, S-wave and D-wave of singly heavy bottom-strange baryons) are analyzed in the heavy hadron chiral perturbation theory(HHChPT), in absence of any experimental result we have compared our results to Ref.⁵⁶ and Ref.⁵⁵ (see Table 11). All results in table are not in mutually agreement with each other. More efforts are required for the decay properties of these baryons(as they are very important for the internal structure of baryons), in both the fronts, experimental as well as theoretical to study these properties to reach out for any conclusion.

In this study, our aim is satisfied for the assignment of J^P value of the experimentally measured resonance states, which can be seen in Figure 4 and model is successful in the determination of the various decay properties of singly heavy bottom-strange baryons. We would like to extend this model for doubly and triply heavy baryons in near future.

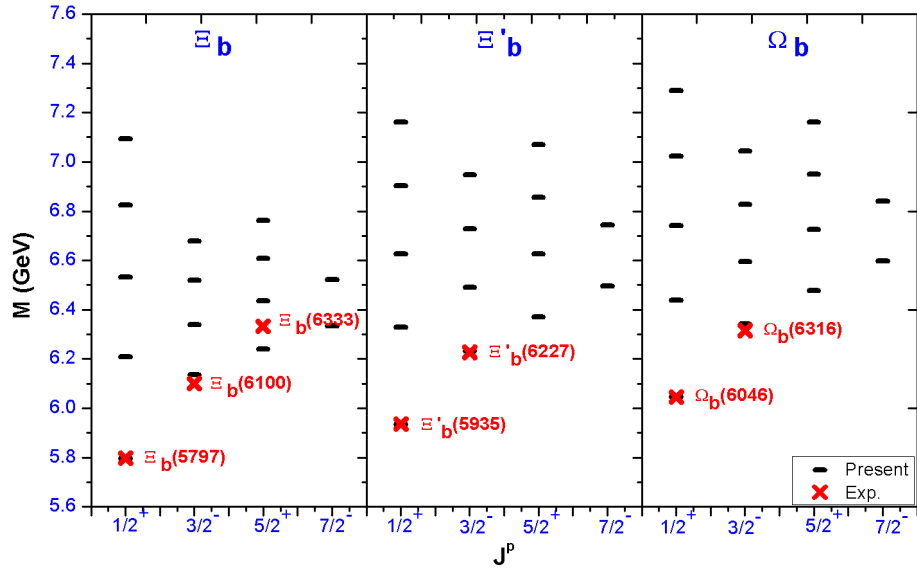


Fig. 4. Mass spectra representation of singly heavy bottom-strange baryons with experimentally detected states

References

1. P. A. Zyla et al. (Particle Data Group), *Prog. Theor. Exp. Phys.* **2020**, 083C01 (2020).
2. LHCb Collaboration (R. Aaij et. al.), *Phys. Rev. D* **103** 1, 012004 (2021).
3. LHCb Collaboration, (R. Aaij et. al.), *Phys. Rev. Lett.* **121**, 072002 (2018).
4. LHCb collaboration, (R. Aaij et. al.), *Phys.Rev.Lett.* **124** 8, 082002 (2020).
5. LHCb collaboration, (R. Aaij et. al.), arXiv:2110.04497v1 [hep-ex] (2021).
6. CMS Collaboration, (A. M. Sirunyan et. al.), *Phys. Rev. Lett.* **126**, 252003 (2021).
7. D. Jia, W. N. Liu and A. Hosaka, *Phys. Rev. D* **101**, 034016 (2020).
8. K. Azizi, Y. Sarac and H. Sundu, *J. High Energy. Phys.* **244** (2021).
9. L. Y. Xiao, K.L. Wang, M. S. Liu, et al., *Eur. Phys. J. C* **80**, 279 (2020).
10. D. Jia, J. H. Pan, C. Q. Pang, *Eur. Phys. J. C* **81**, 434 (2021).
11. S. M. Moosavi Nejada, A. Armat, *Eur. Phys. J. A* **56**, 287 (2020).
12. H. Z. He, W. Liang et. al., *Sci. China Phys. Mech. Astron.* **64**, 261012 (2021).
13. Y. Yamaguchi, S. Ohkoda, et. al., *Phys. Rev. D* **91**, 034034 (2015).
14. Z. Y. Wang, J. J. Qi et. al., *Chin. Phys. C* **41**, 093103 (2017).
15. H. Mutuk, *Eur. Phys. J. A* **56**, 146 (2020).
16. D. Ebert, R. N. Faustov and V. O. Galkin, *Phys. Rev. D* **84**, 014025 (2011).
17. Z. G. Wang, *Int. J. of Mod. Phys. 35*, 2050043 (2020).
18. Q. Mao, H.X. Chen, W. Chen, A. Hosaka, X. Liu and S.L. Zhu, *Phys. Rev. D* **92**, 114007 (2015).
19. B. Chen, K.W. Wei and A. Zhang, *Eur. Phys. J. A* **51** 82, (2015).
20. J. Oudichchya, K. Gandhi, A. K. Rai, *Phys.Rev.D* **104** 11, 114027, (2021); 103 11, 114030 (2021).
21. K. W. Wei et. al., *Phys. Rev. D* **95**, 116005 (2017).
22. J. Sonnenschein and D. Weissman, *Eur. Phys. J. C* **79**, 326 (2019).

23. K. Thakkar, Z. Shah, A.K. Rai and P.C. Vinodkumar, *Nucl. Phys. A* **965**, 57 (2017).
24. W. Roberts and M. Pervin, *Int. J. Mod. Phys. A* **23**, 2817 (2008).
25. A. Valcarce, H. Garcilazo, J. Vijande, *Eur. Phys. J. A* **37**, 217 (2008).
26. Z. Ghalenovi, A. Rajabi, S. x. Qin and D.H. Rischke, *Mod. Phys. Lett. A* **29**, 1450106 (2014).
27. E. Santopinto, *Phys. Rev. C* **72**, 022201 (2005).
28. T. Yoshida et. al., *Phys. Rev. D* **92**, 114029 (2015).
29. K. Chen, Y. Dong, X. Liu, Q.-F. Lü and T. Matsuki, *Eur. Phys. J. C* **78**, 20 (2018).
30. Z. Shah and A.K. Rai, *Few-Body Syst.* **59**, 76 (2018).
31. M. Padmanath and N. Mathur, *Phys. Rev. Lett.* **119**, 042001 (2017).
32. K. Gandhi, Z. Shah and A. K. Rai, *Eur. Phys. J. Plus* **133**, 512 (2018).
33. K. Gandhi, Z. Shah, A. K. Rai, *Int. J Theor. Phys.* **59**, 1129–1156 (2020).
34. A. Kakadiya et. al., arXiv:2108.11062v1 [hep-ph].
35. Z. Shah, A. Kakadiya, K. Gandhi, A.K. Rai, *Universe* **7**, 337 (2021).
36. B. Q. Li and K. T. Chao, *Phys. Rev. D* **79**, 094004 (2009).
37. Z. Shah, K. Thakkar, A. K. Rai, and P. C. Vinodkumar, *Chin. Phys. C* **40**, 123102 (2016).
38. Z. Shah, K. Thakkar, A.K. Rai and P.C. Vinodkumar, *Eur. Phys. J A* **52**, 313 (2016).
39. K. Gandhi, A. Kakadiya, Z. Shah, and A. K. Rai, *AIP Conf. Proc.* **2220** (2020), 140015.
40. A. Kakadiya, K. Gandhi, A. K. Rai, Proceedings of the DAE-BRNS Symp. on Nucl. Phys **64**, 697 (2019).
41. M.M. Giannini and E. Santopinto, *Chin. J. Phys.* **53**, 020301 (2015).
42. R. Bijkar, F. Iachello, A. Leviatan, *Ann. Phys.* **284**, 89 (2000).
43. R. Bijkar, F. Iachello, A. Laviatan, *Ann. Phys. (N. Y.)* **236**, 69 (1994).
44. M. B. Voloshin, *Prog. Part. Nucl. Phys.* **61**, 455 (2008).
45. J. Z. Wang, D. Y. Chen, X. Liu, T. Matsuki, *Phys. Rev. D* **99**, 114003 (2019).
46. W. Lucha and F. Schoberls, *Int. J. Mod. Phys. C* **10**, 607 (1999).
47. M. Karliner and J. L. Rosner, *Phys. Rev. D* **92**, 074026 (2015).
48. K.A. Olive, *Chin. Phys. C* **38**, 090001 (2014).
49. LHCb collaboration, (R. Aaij et. al.), *Phys. Rev. Lett.* **114** 062004 (2015).
50. LHCb collaboration, (R. Aaij et. al.), *Phys. Rev. Lett.* **113**, 032001 (2014).
51. CMS collaboration, (S. Chatrchyan et al.), *Phys. Rev. Lett.* **108**, 252002 (2012).
52. LHCb collaboration, (R. Aaij et. al.), *Phys. Rev. D* **93**, 092007 (2016).
53. CDF collaboration, T. Aaltonen et al., *Phys. Rev. D* **80**, 072003 (2009).
54. D0 collaboration, (V. Abazov et. al.), *Phys. Rev. Lett.* **101**, 232002 (2008).
55. A. Limphirat et al., arXiv:0710.3942[hep-ph].
56. A. MAjethiya, *Properties of Heavy Flavour Baryons Using Quark Model* Sardar Patel University, [Thesis].
57. A. Majethiya, B. Patel, P. C. Vinodkumar, *Eur. Phys. J. A* **42**, 213 (2009).
58. R. Dhir, C. S. Kim, and R. C. Verma, *Phys. Rev. D* **88**, 094002 (2013).
59. B. Patel, A. K. Rai and P. C. Vinodkumar, *J. Phys. G* **35** 065001, (2008) [J. Phys. Conf. Ser. 110 (2008) 122010].
60. A. Bernotas and V. Simonis, *Lith. J. Phys.* **53**, 84 (2013).
61. J. Franklin, D. B. Lichtenberg, W. Namgung, and D. Carydas, *Phys. Rev. D* **24**, 2910 (1981).
62. D. Pirjol, T. M. Yan, *Phys. Rev. D* **56**, 5483 (1997).
63. H. Y. Cheng, C. K. Chua, *Phys. Rev. D* **75**, 014006 (2007).
64. H. Y. Cheng, C. W. Chiang, *Phys. rev. D* **95**, 094018 (2017).
65. H. Y. Cheng and C. K. Chua, *Phys. rev. D* **92**, 074014 (2015).

20 *Amees Kakadiya, Zalak Shah and Ajay Kumar Rai*

66. Wuensch K L 2011 *Chi-Square Tests* (Berlin: Springer) pp 252–53.